Effect of strain on the band structure of $In_xGa_{1-x}As$

A. Stampfl, X. D. Zhang, G. Kemister, R. C. G. Leckey, and J. D. Riley
Department of Physics, La Trobe University, Bundoora, Victoria 3083, Australia

B. Usher and P. T. Orders
Telecom Research Laboratories, Clayton, Victoria 3168, Australia

R. Denecke, J. Faul, and L. Ley
Institut fur Technische Physik, Universitat Erlangen/Nurnberg, Erwin Rommel Strasse, D-8520 Germany
(Received 2 July 1991)

Angle-resolved photoemission measurements from normal-emission spectra have been used to determine the strain-induced changes in shape of the valence bands of $In_xGa_{1-x}As$ alloys with In concentrations of 10%, 20%, 27%, and 30%. The data have been analyzed using an iterative technique in which the experimentally determined bulk bands are fitted by polynomials. Differences between the strained and unstrained bands show **k**-dependent shifts that are similar in all alloys studied and whose sign and magnitude have been reproduced in the calculations. We observe an increasing strain-induced shift with concentration as reported but the shift is of the opposite sign to that previously reported by other investigators.

I. INTRODUCTION

Interest in the semiconductor III-V system InAs-GaAs arises from the desire to control the band gap and electronic properties of materials which can be used as base materials for lasers and detectors optimally matched to optical fibers. The electronic properties and lattice constant of these materials may be changed by altering the relative cation concentrations. The InAs-GaAs system encompasses a band-gap range from 0.36 to 1.42 eV, making it a likely contender as infrared optoelectronic devices operating between 1.3 (0.95 eV) and 1.55 μm (0.80 eV). There is a 7% difference between the lattice constants of the constituent compounds, which means that the growth of $In_xGa_{1-x}As$ on GaAs, for example, causes the initial layers of molecular-beam epitaxy (MBE) grown material to be strained. This strain has interesting consequences in thin-layer superlattices in that control of the band gap can be accomplished by varying the [In]/[Ga] ratio, but it can also have detrimental effects on the performance of the material in devices.

$In_xGa_{1-x}As$ grown on GaAs causes the alloy to be compressively strained perpendicular to the direction of growth. As the thickness of the layer is increased, defects are introduced which relieve the strain until the equilibrium lattice constant characteristic of the alloy is achieved. This relaxation process has been characterized by a critical thickness, the maximum thickness which maintains the substrate lattice spacing and hence the strained layer. The transition to the unstrained state is not abrupt, however, and the strain is progressively relieved by the introduction of defects even in thin layers. Care is therefore required in the estimation of the actual strain in such ternary alloys.

Photoelectron-spectroscopic measurements of strained systems have shown that valence-bands shift and that effective masses are altered in systematic ways as a function of strain.[1-3] Theoretical studies have reproduced the major trends in these results.[4] Hwang *et al.*[3] compared their experimentally determined band structure for a strained lattice ($In_xGa_{1-x}As$ on GaAs) with that of an unstrained system in the Γ-X direction. They found that the dispersion of the upper three valence bands was reduced in the strained alloy and that the shifts observed in individual bands were **k** dependent. Our own measurements[5] showed similar **k**-dependent shifts, but they were of opposite sign to those reported by Hwang *et al.*[1]

In this paper we report the results from a number of measurements on $In_xGa_{1-x}As$ alloys in both strained and unstrained form for four values of x, namely $x=0.10,0.20,0.27,0.30$. The measurements were designed to test the **k** dependence of the strain-induced changes in the valence-band structure and to confirm the direction of the shift with strain. Particular care was taken to minimize the variability of experimental parameters between measurements on the strained and unstrained alloys. A large number of angle-resolved ultraviolet photoemission spectroscopy spectra were acquired using a p-polarized synchrotron radiation with photon energies between 11 and 70 eV. Data were acquired for polar angles which covered the complete range of $\pm 90°$ using a toroidal analyzer[6,7] connected to the TGM4 beamline at the BESSY synchrotron light source in Berlin.

Effect of strain

The ternary alloy $In_xGa_{1-x}As$ is crystalline with the symmetry of the constituent compounds, but the distribution of the In and Ga on the cation sites is random with an occupation probability proportional to the relative concentrations. Since the In-As bond is longer than the average lattice constant and the Ga-As bond is shorter

TABLE I. Elastic constants for constituent compounds.

	InAs	GaAs
C_{11}	8.33	11.88
C_{12}	4.53	5.38
σ	0.352	0.312
Lattice constant a	6.0584 Å	5.6533 Å

than average, the final arrangement will be a slightly distorted form of the ideal zinc-blende structure with bond lengths and angles controlled by minimization of the local elastic energy.

No theoretical band structures for either the strained or unstrained $In_xGa_{1-x}As$ random alloys have been produced due to the difficulty in using single-cell potentials randomly distributed through the lattice. This means that it is not possible to make a comparison between theory and an experimental band structure. Several models exist, such as the simple virtual-crystal model based on an average potential and the more sophisticated coherent-potential approximation. These have produced densities of states for random alloys. Ling and Miller[8,9] have used single-cell methods by taking a weighted average of all possible configurations of the constituents to produce band structures for $InAs_{1-x}Sb_x$ and to estimate the changes in binding energy of critical points in $In_xGa_{1-x}As$ and $Al_xGa_{1-x}As$ as a function of composition. The calculations of Zollner *et al.*[4] on the effect of strain on GaAs are, however, the only calculations available for comparison with the experimental results reported here.

The lattice constant of GaAs is 5.65 Å and that of InAs is 6.06 Å, as given in Table I, which also shows the elastic constants C_{11} and C_{12} and the Poisson ratio σ. The equilibrium lattice constant of the ternary alloy $In_xGa_{1-x}As$ follows Vegard's law, with the equilibrium lattice constant scaling as the concentration of the constituent alloys. Thus the equilibrium lattice constant for the values of x used are given in Table II, which shows that the equilibrium lattice constant for the alloys is larger than the GaAs lattice constant. An $In_xGa_{1-x}As$ alloy grown on a GaAs substrate is therefore under compression in both directions parallel to the sample surface which results in a tensile strain in the direction normal to the surface. The lattice constant in the normal direction can be measured from thick relaxed samples, but for the thinner strained layers this is not possible, so elastic theory is used. The lattice constant in the normal direction $a_\perp$ is given by the equation[10]

$$a_\perp = a_{eq} + \frac{2\sigma}{1-\sigma}(a_{eq} - a_\parallel) ,$$

where a_{eq} is the equilibrium lattice constant, σ is the Poisson ratio given by $C_{12}/(C_{11}+C_{12})$, and $a_\parallel$ is the lattice constant in the surface. The Poisson ratio for the alloys is also considered to obey Vegard's law.

The relationship between the basis vectors $\mathbf{a}_i'$ in the strained and $\mathbf{a}_i$ in the unstrained lattice is given by $\mathbf{a}_i' = \mathbf{a}_i \cdot (1+\varepsilon)$ where ε is the strain tensor. The strain can be treated as a transformation of coordinates such that the Hamiltonian of the strained system is a coordinate transformation of the unstrained Hamiltonian.[11] Comparison of the bands should therefore be made using $\mathbf{k}$ values normalized to the Brillouin-zone boundaries of each lattice.

The alloy symmetry changes from the zinc-blende structure of GaAs, point-group symmetry T_d, to body-centered tetragonal whose primitive translation vectors are similar to those of a fcc lattice. The idealized point group becomes D_{2d} with a consequent reduction of symmetry at some high-symmetry points in the Brillouin zone. There is no effect of this reduction in symmetry on the degeneracies of the bands along the principal directions from those determined for the T_d double group needed for the spin-orbit interaction. The character tables of the double groups for T_d and D_{2d} are given in the Appendix with the representational decompositions at Γ and Z.

II. EXPERIMENT

A. Crystal growth and characterization

The $In_xGa_{1-x}As$ layers were grown on (100)-oriented GaAs substrates by MBE using a Varian 310 system. The GaAs substrate was heated to 620 °C in a flux of arsenic for approximately 5 min in order to establish an atomically clean and well-ordered surface prior to the growth of a 0.2-mm-thick GaAs buffer layer. The GaAs buffer layer was probably 0.25 μm. The ternary layer was grown at 520 °C under As-stabilized conditions. The growth rate (1.05 μm h^{-1}) and thickness were determined by reflection high-energy electron diffraction intensity oscillation measurements. The substrate was rotated continuously during growth so as to minimize any inhomogeneity in the [In]/[Ga] ratio arising from spatial variations in the In and Ga flux distributions. After growth the sample was cooled by mechanically coupling a

TABLE II. Lattice constants for ternary alloys.

	$In_{0.10}Ga_{0.90}As$	$In_{0.20}Ga_{0.80}As$	$In_{0.27}Ga_{0.73}As$	$In_{0.30}Ga_{0.70}As$
σ	0.316	0.320	0.323	0.324
a_{eq}	5.693 Å	5.734 Å	5.763 Å	5.773 Å
$a_\parallel$	5.653 Å	5.653 Å	5.653 Å	5.653 Å
$a_\perp$	5.730 Å	5.811 Å	5.868 Å	5.888 Å
$\perp$ strain %	0.65	1.34	1.82	2.03

TABLE III. Epilayer thicknesses of samples used in this study.

Sample thickness	Unstrained (μm)	Strained (Å)
$In_{0.10}Ga_{0.90}As$	1.0	50
$In_{0.20}Ga_{0.80}As$	0.75	30
$In_{0.27}Ga_{0.63}As$	0.4	80
$In_{0.30}Ga_{0.70}As$	1.0	20

liquid-nitrogen-cooled finger to the molybdenum block on which the sample was mounted. A thick passivating layer of amorphous As was deposited over the surface of the sample over 1–2 h at an As background pressure of 4×10^{-5} Torr.

The In mole fraction values (x) were determined from the average $In_xGa_{1-x}As$-GaAs peak separation in x-ray rocking-curve measurements performed at four x-ray azimuthal angles using a double-crystal diffractometer on a completely relaxed sample. Details of the samples used in this study are given in Table III.

A strained system such as the $In_xGa_{1-x}As$ ternary alloys grows initially with the lattice constant of the substrate, but as the thickness increases, defects form and threading dislocations are able to glide and elongate in the subsequent layers and so relieve the stress. This growth model has been characterized by a critical thickness, below which the lattice grows in the strained condition and beyond which the process of dislocation development begins. Matthews and Blakeslee[12] (MB) have modeled the relief of the strain due to pre-existing or grown-in dislocations in the substrate and hence determined the critical thickness as a function of In concentration. Measurements on $In_xGa_{1-x}As$ alloys of different compositions grown on crystalline substrates with a small number of defects[13] have shown that the observed thickness at which significant changes of the lattice constant are observed, is considerably larger than the predictions of this MB high defect model. It is believed that many dislocations are created before the x-ray measurements can detect their presence. For example, for the $x=0.27$ alloy, the MB model predicts a critical thickness of 40 Å and a relief of 40% of the strain at 80 Å. For the samples with $x=0.27$ the actual grown-in dislocations are expected to be less than those on which the MB model is based, so the strain in the sample will lie between the full strain of 1.9% and the 1.2% strain predicted by MB model.

B. Ultraviolet photoelectron measurements

The samples were heated in a preparation chamber, whose base pressure was 2×10^{-10} mbar, to remove the As overlayer. The As evaporates at temperatures above about 100 °C, with the rate depending exponentially on temperature. The surface was transformed from an unreflecting milky appearance to a highly reflecting state characteristic of the MBE-grown material. The cleanliness was confirmed both by the observation of low-energy electron diffraction patterns and by the photoelectron spectra at a photon energy around 30 eV, where the escape depths are small and the spectra are particularly sensitive to contamination.

The samples were transferred under ultrahigh vacuum to the analyzer chamber whose pressure remained close to 2×10^{-10} mbar during the measurement time. The spectra showed a slight deterioration after three days in this chamber. The toroidal analyzer[6] used for the photoelectron measurements accepts electrons with polar angles $-90°$ to $+90°$ at one azimuthal angle defined to within $\pm1°$. The resolution in the polar plane was $\pm1.0°$ and the energy resolution of the analyzer and monochromator was 0.2 eV. The analyzer chamber was connected to the TGM4 monochromator on the BESSY storage ring in Berlin whose photon energy range is 10–130 eV using two gratings. To obtain a calibration of the polar angle a movable aperture can was lowered to block the entrance slit except for holes at 30° intervals. A spectrum was then taken whose angular distribution is a series of peaks with 30° separation which were used to calibrate all other spectra from that particular sample.

For the measurements on the sample with an In fraction of 0.27, two separate sets of identical samples were used and the data was taken 3 months apart. The sets of data used in the analysis of both the strained and unstrained data[14] are compilations from these two measurements, a single strained or unstrained sample being measured on each occasion. The agreement between the data from these two independent experiments gives us confidence in the reliability of the measurements and in the process for determining energy and **k** values from the data.

In the second and third series of measurements (on the samples with In fraction $x=0.1$, 0.2, and 0.3) the variability of the experimental parameters was further minimized. A sample of the strained alloy and another of the unstrained alloy were mounted in the same sample holder, one "above" the other. They were aligned along the substrate cleavage edges (110) so that the azimuthal directions were identical and the alignment of the surface normals was better than 0.5° as judged by optical reflections from the two sample surfaces. Thus, for each measurement, all experimental parameters were constant with the exception of the rigid translation of the sample manipulator needed to interchange the sample being illuminated.

The monochromator was calibrated by comparing the binding energies of the In and Ga $3d$ core lines. Accurate values of core-level binding energies with respect to the spectrometer vacuum level were obtained from core-level spectra using first- and second-order light at one monochromator setting. Corrections were applied to other spectra to adjust for any calibration error. Spectra were mostly taken at steps of 1 eV for photon energies from 11 to 30 eV, in steps of 2.5 to 40 eV and in steps of 5.0 eV to a photon energy of 50 eV.

III. RESULTS

A large number of angle-resolved spectra were acquired at azimuthal angles between $+80°$ and $-80°$, but

only data from normal-emission spectra will be discussed in this paper. The energy distribution curves (EDC's) from the $In_{0.27}Ga_{0.73}As$ strained alloy are shown in Fig. 1 in which the transitions to the primary-cone free-electron band are clearly visible. The calculated positions of the core lines for In, Ga, and As due to higher-order light, are shown as arrows in Fig. 1 from which it can be seen that only the As core line has any significant intensity in the valence-band region.

IV. DATA ANALYSIS

Our earlier paper on $In_xGa_{1-x}As$ (Ref. 14) described the process used to determine the valence-band structure of unstrained $In_xGa_{1-x}As$ from angle-resolved photoemission data taken normal to the surface. This process involves the determination of the peak positions in the normal-emission (EDC's) and the use of a structure plot (binding energy against photon energy) for these transitions. This permits identification of primary-cone transitions and of the binding energy and photon energy at which transitions from the top of the valence band at Γ are observed. The inner potential V_0 (referred to the vacuum level) is determined by identifying the photon energy at which transitions from the X point are observed. The perpendicular momentum $k_\perp$ can then be calculated for all other transitions using the free-electron final-state model to give energy and momentum values for the two valence bands.

In simple materials, these bands would be compared with calculated bands to test the agreement between theory and experiment. No calculations of the band structures of the alloys exist, and so we determine empirical bands from the experiment. The free-electron final-state model, implicit in this analysis, applies for photon energies above about 20 eV. Thus transitions from an initial-state band for photon energies above 20 eV and transitions at minimum binding energy, the top of the valence band, are fitted to a fifth-order polynomial constrained to generate a band horizontal at the Brillouin-zone boundary and at Γ. The bands, thus determined, are then used as experimental initial-state bands which are used to generate the "theoretical" structure plot. This enables the identification of umklapp transitions, surface states, and one-dimensional density-of-states effects. In the following description of the analysis of the results from the various alloys, systematic trends are sought and comparisons made, which validate the above process of analysis.

The structure plot generated from the data of Fig. 1 is shown in Fig. 2 with the calculated plot shown as continuous lines. These lines correspond to transitions from the initial state to final states with **G** vectors defined for a tetragonal lattice (see Fig. 3). Similar structure plots were generated using the data from all samples of strained and unstrained $In_xGa_{1-x}As$ alloys and the primary-cone transitions similarly identified. The value of the inner potential V_0 for each alloy was determined from the binding-energy minimum at Z_7 (equivalent to

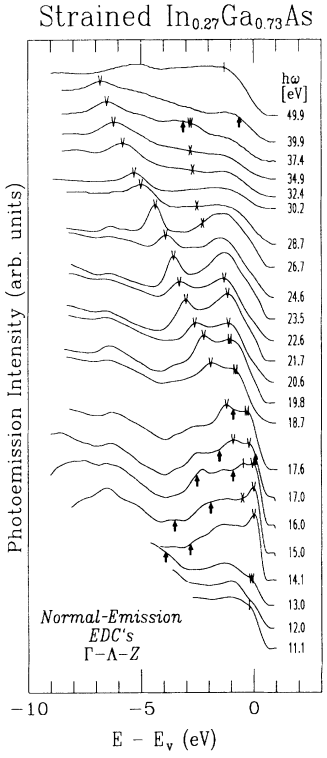

FIG. 1. Normal-emission spectra at labeled photon energies from the (001) surface of the strained $In_{0.27}Ga_{0.73}As$ ternary alloy. Peaks marked with crosses arise from transitions to the primary cone in the free-electron final-state model. Arrows mark the expected positions of the core levels from As, In, and Ga excited by second-order light from the grating. Letter symbols indicate the relative strength of the peaks increasing in the order *X-W-M-I-V*.

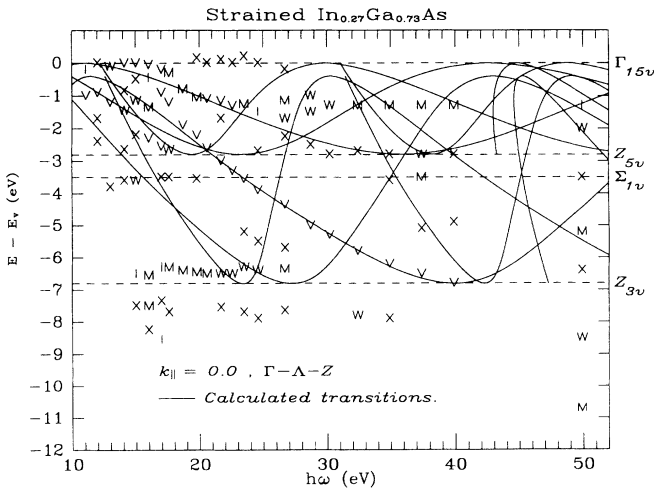

FIG. 2. Structure plot of binding energy against photon energy for peaks in the normal-emission spectra of $In_{0.27}Ga_{0.73}As$ (001) marked with crosses. Letter symbols indicate the relative strength of the peaks increasing in the order *X-W-M-I-V*. The "theoretical" structure plot (— — —) is based on free-electron final states and a polynomial fit to the experimentally derived initial states (Ref. 14).

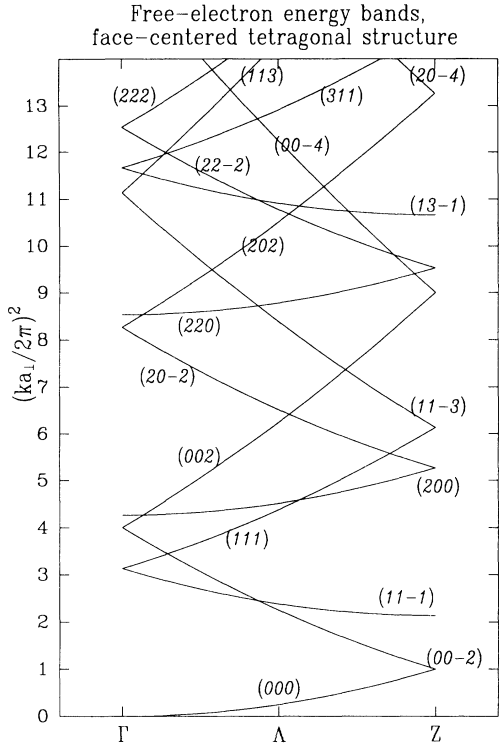

FIG. 3. Free-electron bands for normal emission from the (001) face of strained $In_{0.27}Ga_{0.73}As$. The energy axis has been normalized to the lowest free-electron bandwidth $(\hbar^2/2m)(2\pi/a_\perp)^2$. Each band has been labeled with one G vector, ignoring degeneracies.

X_3 or X_7 in the unstrained GaAs lattice) assuming a transition to a free-electron final state **G** [(0,0,2)] as described above. The inner potential, given in Table IV, for each strained sample is less than that of the equivalent unstrained alloy and reduces with increasing In concentration. The latter observation is consistent with the lower inner potential of InAs relative to GaAs.[15] In all cases the fitting of the data is not very sensitive to the value of V_0 and we estimate that the error in the data of Table IV is about ±0.5 eV.

In fitting the bands, the top of the valence band was chosen at the peak with the lowest observed binding energy. This occurs at a photon energy near 15 eV ($\Gamma_{6v,7v}$). The splitoff band maximum (Γ_{7v}) was chosen using the peak with minimum binding energy associated with that band. This also occurred near 15 eV photon energy. The Γ_{6v}-Γ_{7v} separation should be equal to the spin-orbit splitting observed by other techniques, but the values determined from the present measurements, given in Table V, are larger than the values of the spin-orbit splitting of the constituent compounds given in Ref. 16. The cause of this is unclear. We note that this separation is reduced in alloys for $x > 0.1$.

The experimental initial-state bands were determined for each of the alloy concentrations as binding energy (with respect to the top of the valence band) against **k** and are plotted in Fig. 4. In the discussion below, the band numbers are fixed by counting from the lowest valence band with increasing energy. Thus in semiconductor parlance, the splitoff band is band 2 and the unseparated light-hole and heavy-hole bands are bands 3 and 4.

The effect of strain on the bands is evident in Fig. 4 and several trends can be discerned. The width of band 2 (splitoff band) increases with strain with the band flattening at Γ crossing the unstrained band at an intermediate value of **k** and having a larger binding energy at the Z (X) point. The experimental data for the bands 3 and 4 consists of rather weak, broad peaks with few points being observed for photon energies between 20 and 30 eV. The fitting process depends heavily on these few points and the detailed band shape is therefore not as reliable as for band 2. Trends can still be observed, however, with a reduction of the bandwidth for the 10% alloy (0.65% strain) with strain, equal bandwidths for 20% alloy (1.34% strain), and an increase in bandwidth with strain for the 27% and 30% alloys (1.83% strain).

TABLE IV. Inner potentials, with respect to vacuum, for the alloys used.

Alloy	V_0 (eV)
$In_{0.10}Ga_{0.90}As$ unstrained	14.76
$In_{0.10}Ga_{0.90}As$ strained	13.43
$In_{0.20}Ga_{0.80}As$ unstrained	12.38
$In_{0.20}Ga_{0.80}As$ strained	12.28
$In_{0.27}Ga_{0.73}$ unstrained	12.08
$In_{0.27}Ga_{0.73}$ strained	11.51
$In_{0.30}Ga_{0.70}As$ unstrained	12.02
$In_{0.30}Ga_{0.70}As$ strained	10.50

TABLE V. Observed splittings between heavy-hole band and splitoff band.

Sample	Δ_0 Unstrained	Δ_0 Strained	Δ_0 Optical
GaAs	0.35[5]		0.341
InAs	0.41[5]		0.371
$In_{0.10}Ga_{0.90}As$	0.47	0.48	
$In_{0.30}Ga_{0.80}As$	0.4	0.3	
$In_{0.27}Ga_{0.63}As$	0.55	0.4	
$In_{0.30}Ga_{0.70}As$	0.5	0.43	

TABLE VI. Shifts in the binding energy of critical points in the band structure with strain.

Critical point	Theory GaAs (eV)	Experimental $In_{0.27}Ga_{0.73}As$ (eV)
Γ band 2	−0.15	0.1
$Z_7(X_3)$ band 2	0.41	0.3
$Z_7(X_5)$ band 3,4	0.0	0.1

The strain fields in the alloy can be represented as a hydrostatic compression together with a tensile stress in the growth direction. Zollner *et al.*[4] have used this representation in linear muffin-tin orbital calculation to predict the changes in the band structure of GaAs with strains equivalent to those in $In_{0.27}Ga_{0.73}As$ grown on GaAs. The results of this calculation are shown in Fig. 5 and are summarized in Table VI. In both the theory and the experiment the binding energy of the Z point (X_3 point) for band 2 (the splitoff band) increases—by 0.41 eV in the theory and by 0.30 eV in the experiment. The Γ-point binding energy of this band is observed to decrease in en-

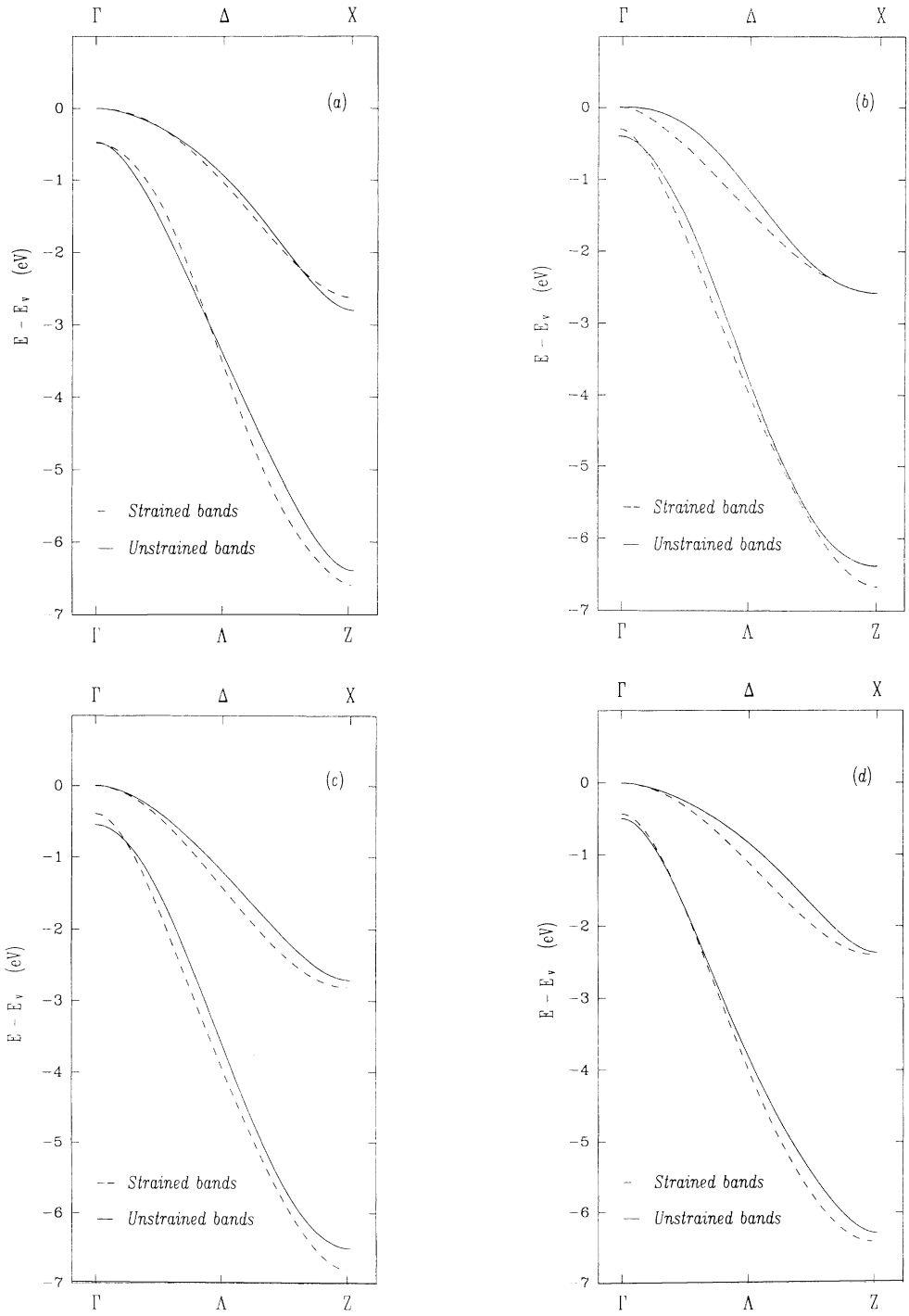

FIG. 4. Comparison of the strained (2) and unstrained (3 and 4) experimentally determined valence bands (the lowest valence band is 1) for (a) $In_{0.10}Ga_{0.90}As$, (b) $In_{0.20}Ga_{0.80}As$, (c) $In_{0.27}Ga_{0.73}As$, (d) $In_{0.30}Ga_{0.70}As$. The bands are plotted relative to the top of the respective valence bands which have been aligned. The k values have been normalized to the Brillouin-zone boundary for each alloy. Dashed lines, strained alloy; solid lines, unstrained alloy.

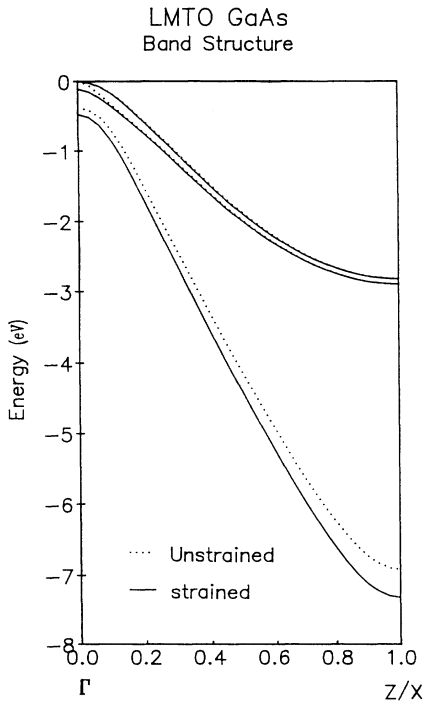

FIG. 5. Band structures of strained (solid lines) and unstrained (dotted lines) GaAs for a combination of hydrostatic and strain equivalent to the strain induced in $In_{0.27}Ga_{0.73}As$ when grown on GaAs (Ref. 18).

ergy by 0.15 eV, while the calculation predicts an increase of 0.1 eV. The calculation predicts no change in the bandwidth of bands 3 and 4, whereas an increase of 0.1 eV is observed for the alloy. The theoretical calculation has therefore predicted the observed direction of the shifts in the bands away from the Γ point and their orders of magnitude. This is a satisfactory result given the limitations in applying calculations on GaAs to an $In_{0.27}Ga_{0.73}As$ alloy and the limitations of the model used in the analysis of the data.

V. CONCLUSION

Angle-resolved photoemission measurements from normal-emission spectra have been used to determine the strain-induced changes in shape of the valence bands of $In_xGa_{1-x}As$ alloys with In concentrations of 10%, 20%, 27%, and 30%. The data have been analyzed using an iterative technique in which the experimentally determined bulk bands are fitted by polynomials.[14] The consistency of trends in the parameters, as a function of strain and composition, derived from the data (such as the inner potential and spin-orbit splitting) confirm the validity of the fitting process.

Differences between the strained and unstrained bands show **k**-dependent shifts which are similar in all alloys studied and whose sign and magnitude have been reproduced in calculations by Zollner *et al.*[4] We observe an increasing strain-induced shift with concentration as reported in Ref. 1 but the shift is of the opposite sign to

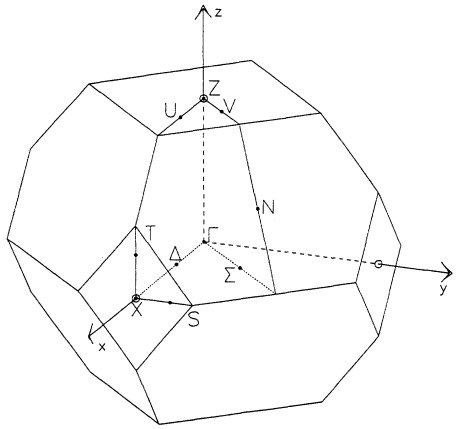

FIG. 6. Brillouin zone of the bond-centered tetragonal lattice of the strained ternary alloys. The change in the *z*-axis direction has been exaggerated.

that reported by Hwang *et al.*[1-3] Our measurements from strained and unstrained samples mounted side by side confirm the sign of the changes reported in our earlier paper.[14]

ACKNOWLEDGMENTS

This work has been supported by the Australian Research Grants Scheme, by the Australian/German Science and Technology Agreement, and by the Bundesministerium für Forschung und Technologie. Thanks are due to the staff of the BESSY synchrotron for their support and hospitality, to Dr. R. Johnson for assistance at critical junctures of the experiment, and to Professor Cardona for encouragement. A.S. and X.Z. thank La Trobe University for partial support.

APPENDIX

The compressive strain in the *x*-*y* plane of the crystal causes tensile strain in the *z* direction which reduces the point group symmetry of the crystal from T_d to D_{2d}. The primitive lattice vectors of the system are changed little except that the *z* components are extended by the tensile strain in the *z* direction. The primitive cell is similarly altered and becomes body-centered tetragonal. The Brillouin zone, shown in Fig. 6, is a compression, in the *z* direction, of the usual face-centered cubic cell. This has the other effect of changing the labeling of the principle directions. Thus the Γ-Δ-*X* direction along a (100) axis in the fcc system becomes a Γ-Λ-*Z* direction in the tetragonal lattice. The group of the wave vector at Δ and Λ is the same, C_{2v}, while at *X* and *Z* the group of the wave vector is D_{2d}. Thus the only possible extra splittings due to the effect of strain may occur at Γ.

The character tables shown are for the groups D_{2d} and T_d from which the compatibility relations between the representations can be determined and hence the likely splittings due to the strain. The analysis is shown first for the single groups, without spin, and then for the double groups, including spin.

D_{2d}	E	C_2	$2S_4$	$2C_2'$	$2\sigma_d$
Γ_1	1	1	1	1	1
Γ_2	1	1	1	−1	−1
Γ_3	1	1	−1	1	−1
Γ_4	1	1	−1	−1	1
Γ_5	2	−2	0	0	0

T_d	E	C_2	$2S_4$	$2C_2$	$2\sigma_d$
Γ_1	1	1	1	1	1
Γ_2	1	1	−1	1	−1
Γ_{12}	2	2	0	2	0
Γ_{25}	3	−1	1	−1	−1
Γ_{15}	3	−1	−1	−1	1

Compatibility relations for T_d and D_{2d}.

T_d	Γ_1	Γ_2	Γ_{12}	Γ_{25}	Γ_{15}
D_{2d}	Γ_1	Γ_3	$\Gamma_1+\Gamma_3$	$\Gamma_2+\Gamma_5$	$\Gamma_4+\Gamma_5$

In the situation where spin-orbit splitting is neglected, the uppermost valence-band state in $In_xGa_{1-x}As$ is the triply degenerate state Γ_{15} which is split by the strain-induced reduction in symmetry to a singlet Γ_4 and a doublet Γ_5 state similar to the states determined by spin-orbit splitting in GaAs. If the spin is taken into effect the double groups should be considered.

T_d	E	R	$8C_3$	$8RC_3$	$3RC_2$, $3C_2$	$6R\sigma_d$, $6\sigma_d$	$6S_4$	$6RS_4$
Γ_1	1	1	1	1	1	1	1	1
Γ_2	1	1	1	1	1	−1	−1	−1
Γ_{12}	2	2	−1	−1	2	0	0	0
Γ_{25}	3	3	0	0	−1	−1	1	1
Γ_{15}	3	3	0	0	−1	1	−1	−1
Γ_6	2	−2	1	−1	0	0	$\sqrt{2}$	$-\sqrt{2}$
Γ_7	2	−2	1	−1	0	0	$-\sqrt{2}$	$\sqrt{2}$
Γ_8	4	−4	−1	1	0	0	0	0

D_{2d}	E	R	RC_2, C_2	$2RC_2$, $2C_2$	$2R\sigma_d$, $2\sigma_d$	$2S_4$	$2RS_4$
Γ_1	1	1	1	1	1	1	1
Γ_2	1	1	1	−1	−1	1	1
Γ_3	1	1	1	1	−1	−1	−1
Γ_4	1	1	1	−1	1	−1	−1
Γ_5	2	2	−2	0	0	0	0
Γ_6	2	−2	0	0	0	$\sqrt{2}$	$-\sqrt{2}$
Γ_7	2	−2	0	0	0	$-\sqrt{2}$	$\sqrt{2}$

Compatibility relationships.

T_d	Γ_6	Γ_7	Γ_8
D_{2d}	Γ_6	Γ_7	$\Gamma_6+\Gamma_7$

The upper valence bands in GaAs are Γ_8 and Γ_7. The strain in $In_xGa_{1-x}As$ causes the Γ_8 state to split into two Kramer's doublets Γ_7 and Γ_6. The Γ_7 state remains as Γ_7. There is a reduction in the degeneracy as the Γ_7 and Γ_6 doublets are not related by time-reversal symmetry as the $\Delta_{3,4}$ bands are in GaAs.

The symmetry at Λ in the strained lattice is the same as at Δ in the unstrained lattice C_{2v}. The compatibility relationships between the single groups C_{2v}, T_d, and D_{2d} are given in texts on group theory and solids,[17] whereas the double groups are left to the readers. The C_{2v} double group character table is given below from which the compatibility relationships involving the double-group representations can be derived.

C_{2v}	E	R	RC_2, C_2	$R\sigma_v$, σ_v	$R\sigma_v'$, σ_v'
Δ_1	1	1	1	1	1
Δ_2	1	1	1	−1	−1
Δ_3	1	1	−1	1	−1
Δ_4	1	1	−1	−1	1
Δ_5	2	−2	0	0	0

Compatibility relations for $In_xGa_{1-x}As$.

T_d	Γ_6	Γ_7	Γ_8
$D_{2d}(\Gamma)$	Γ_6	Γ_7	$\Gamma_6+\Gamma_7$
C_{2v}	Λ_5	Λ_5	Λ_5,Λ_5
$D_{2d}(Z)$	Z_6	Z_7	Z_6+Z_7

[1]J. Hwang, C. K. Shih, P. Pianetta, G. D. Kubiak, R. H. Stulen, L. R. Dawson, Y. C. Pao, and J. S. Harris, Jr., Appl. Phys. Lett. **52**, 308 (1988).

[2]J. Hwang, P. Pianetta, G. D. Kubiak, R. H. Stulen, C. K. Shih, Y. C. Pao, Z. X. Shen, P. Lindberg, and B. Chow (unpublished).

[3]J. Hwang, P. Pianetta, L. R. Dawson, G. D. Kubiak, and R. H. Stulen (unpublished).

[4]S. Zollner, U. Schmid, C. Grein, N. Christensen, M. Cardona, and L. Ley (unpublished).

[5]A. Stampfl, G. Kemister, R. C. G. Leckey, J. D. Riley, P. O. Orders, F. U. Hillebrecht, and L. Ley, Phys. Scr. **41**, 617 (1990).

[6]R. C. G. Leckey and J. D. Riley, Appl. Surf. Sci. **22/23**, 196 (1985).

[7]R. C. G. Leckey, J. D. Riley, and A. P. Stampfl, J. Electron Spectrosc. Relat. Phenom. **52**, 855 (1990).

[8]M. F. Ling and D. J. Miller, Phys. Rev. B **34**, 7388 (1986).

[9]M. F. Ling and D. J. Miller, Phys. Rev. B **38**, 6113 (1988).

[10]I. S. Sokolnikoff, *Mathematical Theory of Elasticity* (McGraw-Hill, New York, 1946).

[11]G. L. Bir and G. E. Pikus, *Symmetry and Strain Induced Effects in Semi-conductors* (Wiley, New York, 1974).

[12]J. W. Matthews and A. E. Blakeslee, J. Cryst. Growth **27**, 118 (1974).

[13]B. Usher (unpublished).

[14]A. Stampfl, G. Kemister, R. C. G. Leckey, J. D. Riley, P. O. Orders, B. Usher, F. U. Hillebrecht, J. Fraxedas, and L. Ley, J. Vac. Sci. Technol. A **7**, 2525 (1989).

[15]B. I. Lindqvist, Phys. Status Solidi **32**, 273 (1969).

[16]K.-H. Hellwege in *Semiconductors: Physics of Group IV and III-V Compounds,* edited by O. Madelung, Vol. III/17a Group III: Crystal and Solid State Physics (Springer-Verlag, Berlin, 1982).

[17]J. C. Slater, *Quantum Theory of Molecules and Solids* (McGraw-Hill, New York, 1965), Vol. III.

[18]S. Zollner, U. Schmid, N. E. Christensen, C. H. Grein, M. Cardona, and L. Ley, in *Proceedings of the International Conference on Semiconductors, Thessalonki, 1990,* edited by E. M. Anastassakis and J. D. Joannopoulos (World Scientific, Singapore, 1990).